CAVITATION EFFECT ON THE NEAR NOZZLE SPRAY DEVELOPMENT IN HIGH PRESSURE DIESEL INJECTION.

Ralph Saliba, Ihab Baz, Jean-Claude Champoussin, Michel Lance, Jean-Louis Marié

Ecole Centrale de Lyon, LMFA UMR CNRS 5509, B.P. 163, 69131 Ecully Cedex, France
Tel : (33) 0 4 72 18 61 47 ; Fax : (33) 0 4 78 33 31 10
E-Mail : Ralph.Saliba@ec-lyon.fr

ABSTRACT

Laser light sheet and shadowgraphy techniques have been applied to investigate cavitation phenomena in the spray hole of Diesel injector. The nozzle was supplied with diesel test oil by a Common Rail injection system up to 70 Mpa and discharged into a transparent chamber pressurized up to 5 MPa. The optical techniques allowed us to make a qualitative characterization of cavitation by direct observations and also a quantitative one in statistical term. The local positions of cavitation films, lying between the flow and the nozzle wall as well as those of single bubbles have been observed at different instants of the injection process, and their effect on the spray development has been pointed out. During the cyclic injection process (transient and quasi - stationary phases), the mutual relationship between the development of cavitation within the orifice (position and rate) and the spray angle, were studied according to the dynamics of the needle lift, the injection pressure and the backpressure. Also, results were discussed according to cavitation number and Reynolds number estimated from direct measurements of nozzle sac pressure and injection flow rate.

INTRODUCTION

The spray characteristics and therefore the atomisation behaviour are decisive for Diesel engine performance and pollutants formation. A thorough understanding of the internal flow physics inside the nozzle is fundamental for predicting spray development. The phenomena of the spray breakup in the atomization regime is still not fully understood, because of the complex flow structure interacting with physical effects like cavitation, partial fuel evaporation within the nozzle, and at least, the spray breakup outside the nozzle due to collapsing cavitation bubbles, separation of droplets or ligaments partly under the influence of entrained air [1].

Cavitation has been identified to occur in high pressure Diesel injector nozzles. In terms of multi-phase flow the relative magnitude of the injection and back pressure together with the nozzle and needle geometry and the fuel vaporisation pressure may be used to characterize the flow in the nozzle, excluding the effects of the dissolved gases in the fuel [2-4]. According to the magnitudes of these quantities, the nozzle may present cavitating or non-cavitating flow. The cavitation number based on the relative pressure level characterizes the phenomenon [2] and is given by:

$$K = \frac{P_s - P_b}{P_b - P_v} \tag{1}$$

where P_s is the nozzle sac pressure upstream to the flow orifice, P_v is the vaporisation pressure of the fuel and P_b is the downstream pressure. As the fuel injection process is transient, the flow within the nozzle may switch from non-cavitating to cavitating more than once during the injection period depending on the instantaneous injection pressure and the flow instabilities for a fixed backpressure.

Heimgärtner and Leipertz [1] have studied the influence of the nozzle geometry on the flow close to the nozzle hole exit for different rail and ambient pressures, during the quasi-stationary phase of the injection cycle at full needle lift. They have characterized and compared the behaviour of the microscopic and the macroscopic spray cone angle.

Blessing and *al.* [5] have studied the influence of the conical hole shape and rounded inlet contour on the internal flow and the spray propagation near the nozzle outlet. They have found that the micro-spray angle reaches a maximum during the needle opening and the needle closing, and an approximately constant cone angle is achieved when the needle is fully opened, and thus for different hole geometries. They also found that the decreasing of the conical shape of the spray hole leads to an increased spray angle in combination with a reduced penetration depth.

This work constitutes a contribution to the experimental characterisation of the cavitation existing in high speed flows within the nozzle and its influence on the spray development near the nozzle exit. It extends the previous works by focusing on the effect of the cavitation (location and rate) on the spray angle according to the instantaneous cavitation number (calculated from the measured sac pressure) and Reynolds number.

EXPERIMENTAL SETUP

For investigating the internal flow under diesel injection-like conditions, a standard transparent nozzle is used. The nozzle tip is replaced by an optically polished quartz or an acrylic glass modelling a sac and spray hole (Fig. 1). The orifice has a diameter of 0.4 mm and an l/d ratio of 4.5.
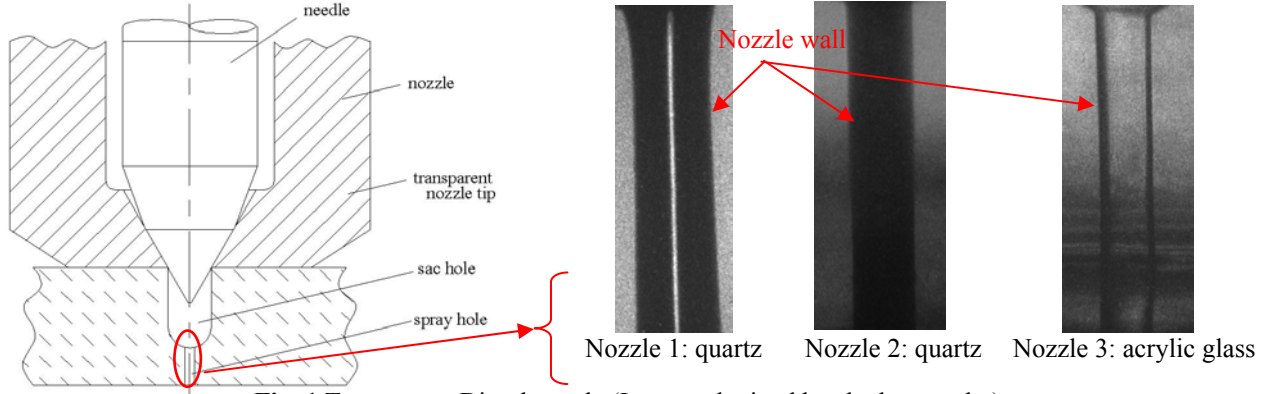

Nozzle 1: quartz   Nozzle 2: quartz   Nozzle 3: acrylic glass

Fig. 1 Transparent Diesel nozzle (Images obtained by shadowgraphy).

The fluid used is the normalized testing oil ISO 4113 with physical properties (density, viscosity and surface tension) identical to those of Diesel fuel, and particularly its refractive index n matches well to that of quartz ($n_{oil}=n_{quartz}=1.46$). Thus, reflection and refraction, when the light passes through the internal surface of the quartz nozzle, are minimized. The experiments were conducted using a Bosch Common-Rail injection system providing real unsteady Diesel injection conditions. The flexibility of this system allows adjusting the injection time and pressure, as well as the number of injection sequences. High rail pressures decrease the lifetime of the quartz nozzle tip. For this reason, all our experiments are carried out at rail pressures small than 50 MPa and with energizing time of 2 ms. The oil is injected into a constant volume transparent chamber capable of carrying high pressures (8 MPa) and with a facility to visualize the interface hole-spray simultaneously. The complete experimental setup is shown in figure 2.

Three mechanical variables are recorded instantaneously. A micro-epsilon sensor gives the needle lift. Goney and al. [6] made an indirect measurement of the sac pressure by detection of the deformation of the nozzle wall by a strain gage. In this work, a direct measurement of the sac pressure is made by using an AVL pressure transducer mounted on an injector tip drilled in steel and having the same dimensions as the transparent one. At last, an EVI flow meter gives the instantaneous injection flow rate. The optical diagnostic system consists of a long-distance microscope and an intensified CCD camera (CCD-chip 1280x1024 pixels). To reduce the blurring effects caused by high flow velocities of more than 150 m/s, an exposure time of 20 ns is used. The light sources used, are a xenon arc lamp for shadowgraphy, and an Argon-ion Laser with an optical setup to produce a light sheet thickness of less than 30 μm for tomography (Fig. 3). Taking into account the small shot to shot fluctuations, especially at the start and the end of injection, an averaged image was calculated from a set of images recorded for every parameter setting at different instants t_a [4]. The cavitation rate was estimated from 60 tomography images taken with the transparent hole discharging in the EVI flow meter, and the spray angle from only 10 shadowgraphy images (actual limitation due to the spray deposit) when it is mounted on the backpressure chamber.
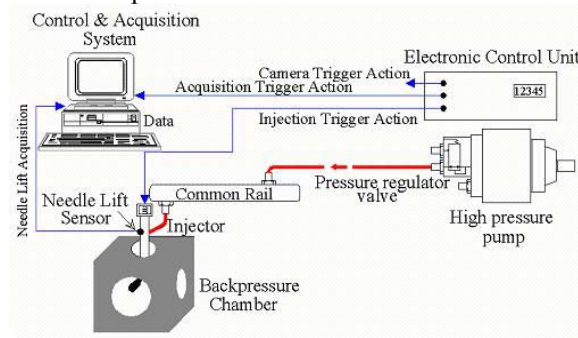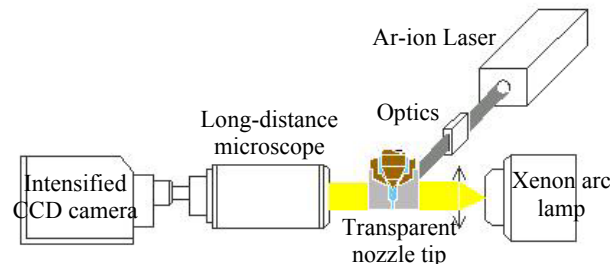

Fig. 2 Experimental facility.

Fig. 3 Optical setup for shadowgraphy and tomography.

RESULTS AND DISCUSSION

In this section, from data acquisition and images gained with the transparent nozzles, investigations are performed first on instantaneous mechanical variables and then, using the image processing, on the dependence of the cavitation rate and spray angle on the inception of the cavitation and its growth with the Reynolds and the cavitation numbers.

Instantaneous Measurements

The flow velocity through the nozzle is mainly affected by the feed pressure and the needle lift. By changing the rail pressure, the dynamic of the needle opening and closing is different (Fig. 4). Therefore, the sac pressure depends on the rail pressure and the needle lift. A small delay between the needle lift start and the sac pressure increase is detected. This delay decreases with increasing the rail pressure. The evolution of the cavitation number (Eq. (1)) presented in figure 5, is calculated from the sac pressure measurement. It can be observed that during the needle opening, its slope increases with increasing rail pressure (Fig 5-a). The cavitation number presents two critical values ($K = K_{crit}$), one at the moment of the inception of the cavitation in the orifice and the other at the moment of its disappearance. The Reynolds number is calculated from flow velocity measurement carried out thanks to the injection rate measurement by the EVI flow meter, and is given by:

$$\mathrm{Re} = \frac{d.V}{\nu} \qquad (2)$$

P_R = 30 MPa ; steel nozzle P_R = 50 MPa ; steel nozzle
Fig. 4 Needle lift, sac pressure and rail pressure during the injection cycle: P_b = 3 MPa, t_e = 2ms.

a P_R = 30; 50 Mpa, P_b = 3 MPa ; steel nozzle   **b** P_R = 30 MPa, P_b = 1 Mpa ; nozzle 3
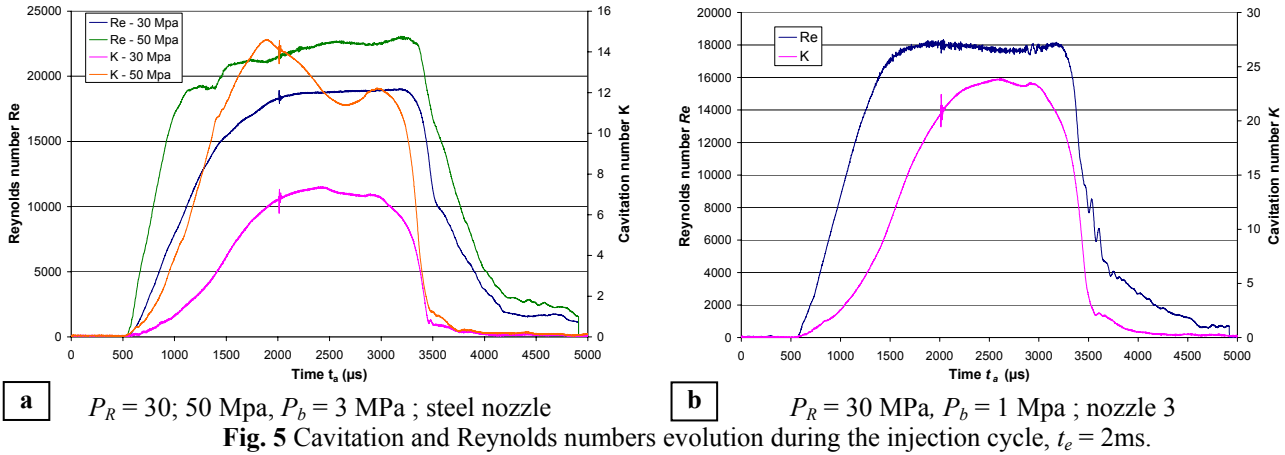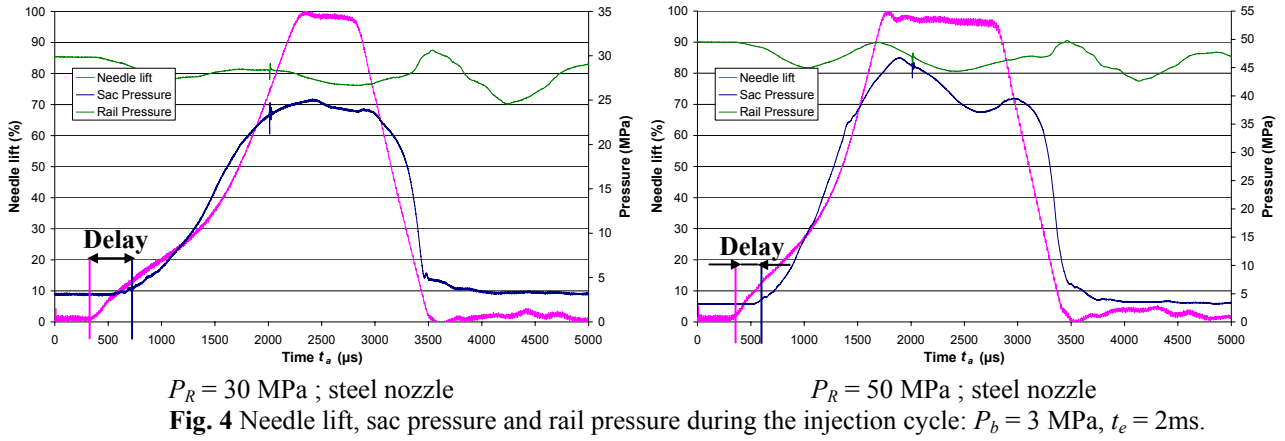**Fig. 5** Cavitation and Reynolds numbers evolution during the injection cycle, t_e = 2ms.

Figure 5-b represents the evolution of Re and K in the same experimental conditions as the shadowgraphy images in figure 6. These shadowgraphy images did not provide an axial section but a projection of the complete cavitation area in the spray hole and of the spray. At the beginning of the injection phase, the gas bubbles sucked in the sac hole and the liquid are pushed out together and expand in the chamber because of lower ambient pressure. The liquid column at the hole exit is influenced by the expansion forces which leads to the mushroom-like shape (Fig 6-a). The tip of the mushroom is the first to be atomized whereas at the nozzle exit one notices the presence of a liquid core inside the spray. The abrupt flow area decrease at the nozzle inlet creates very high flow velocity, which in turn creates a low pressure region near the nozzle inlet [4]. Thus, the cavitation region begins at the inlet corner of the nozzle (Fig 6-b), and when the needle is fully opened, it develops within the spray hole (Fig 6-c and 6-d). As seen in these images, the spray is larger and more atomized on the same side of the cavitation region in the spray hole. An explanation given by modelling in [7] is that this effect is enhanced by the primary break-up process, which is asymmetric due to inhomogeneous distribution of turbulence parameters in the nozzle orifice. During the needle closing, due to the

3

gradual throttling of the fuel flow, the atomization of the spray becomes very poor. This is especially true towards the end of the closing, where the sac pressure becomes very low (Fig. 6-e).
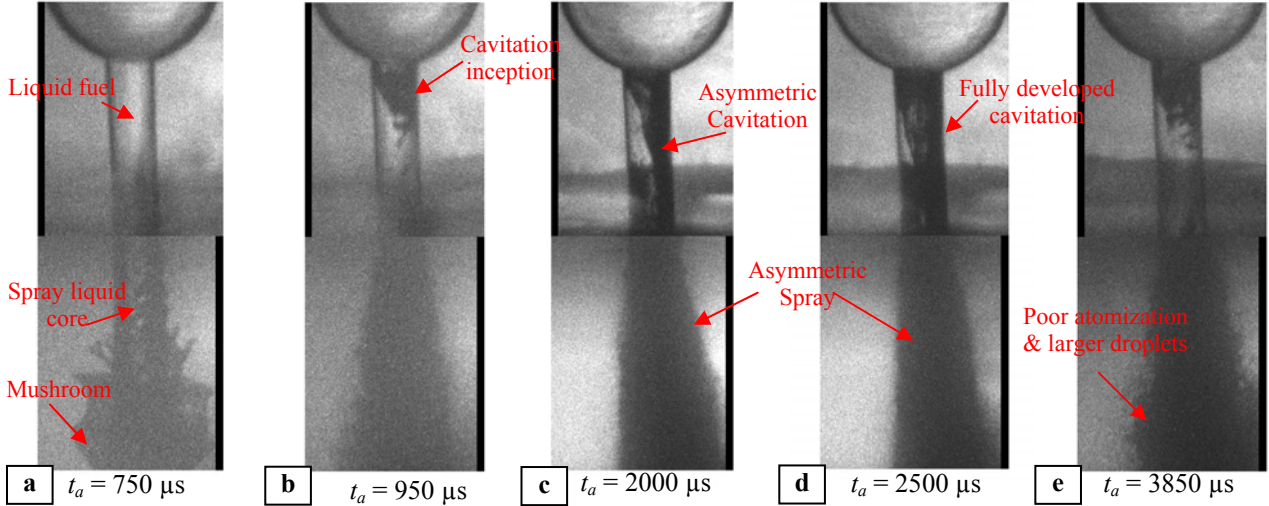

Fig. 6 Spray development under unsteady pressure conditions: P_R = 30 MPa, P_b = 1 MPa, t_e = 2 ms, (Instantaneous images obtained by shadowgraphy with nozzle 3).

Cavitation Rate

The cavitation rate S_C/S_T is defined by Baz [4], as the ratio in the axial section of the orifice, of the average cavitation surface S_C on the total surface of the flow S_T. In other words, it is the surface occupied by the vapour compared to the total surface of the flow in the injection orifice. By fixing the rail pressure and the backpressure, the instantaneous sac pressure, and the type of the flow (monophasic or diphasic) will depend only on the instantaneous position of the needle during the injection cycle. Figure 7 shows the evolution of the cavitation flow pattern and of the cavitation rate during the injection cycle. During the needle opening, cavitation appears strongly in the spray hole and occurs in form of thick films extending from the wall up to the orifice centre and the cavitation rate reaches its maximum. With increasing the rail pressure, the maximum of the cavitation rate is greater and is reached earlier, as figure 7-b shows. It matches well with the evolution of the cavitation number previously observed in figure 5-a. This is due to the fact that by increasing P_R, the needle opens more rapidly and this acceleration of the needle dynamic causes an abrupt flow turbulence increase which amplifies the cavitation. Starting approximately from 70 % of the maximum needle lift, with increasing Reynolds number, the cavitation film which appears in the vicinity of the wall becomes thinner and consequently the effective section of the liquid flow increases. By increasing Re, the time of residence of the bubbles in the flow decreases, consequently the bubbles do not have time to link between themselves to form pockets of cavitation allowing the widening of films of cavitation. These bubbles are carried away with liquid intact core inside the flow and are mainly accumulated at the nozzle exit. In this phase, the cavitation rate decreases considerably. Once the needle is fully opened, the effect of its dynamic can be excluded, and the flow is quasi – stationary: Reynolds and cavitation numbers are stable. One notices that the cavitation rate is almost the same for a fixed backpressure and for different rail pressures (Fig 7-b). The effect of the dynamic of the needle reappears immediately at the beginning of its closing. The influence of the movement of the needle, and the Re decrease support the increase in dimensions of the zone of cavitation and its progressive diffusion towards the centre of the flow. The cavitation rate reaches its second maximum (Fig. 7-b).
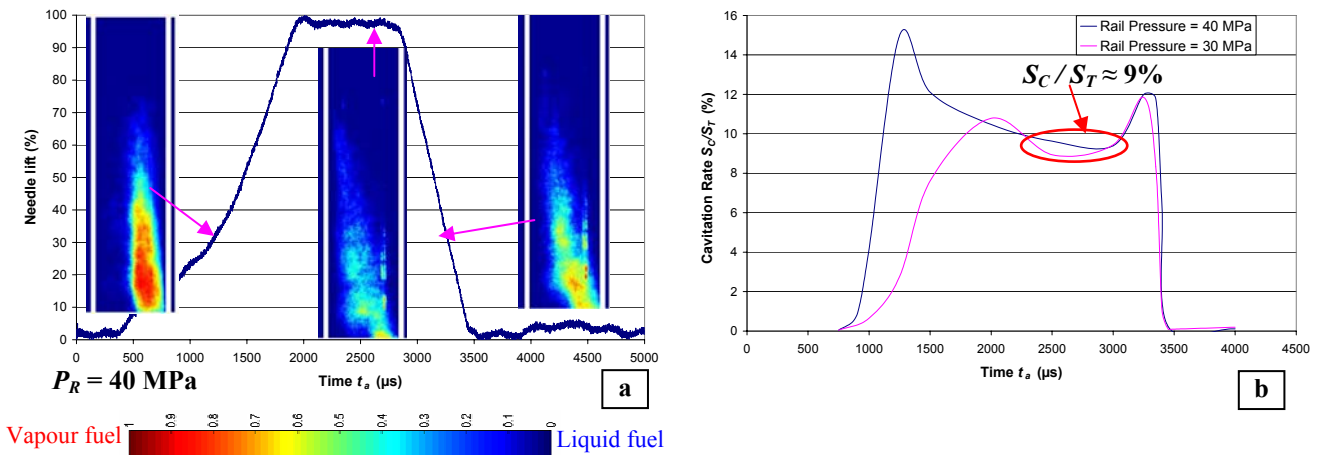

Fig. 7 Probability of existence of cavitation inside the spray hole (a) and Cavitation rate (b) during the injection cycle, P_b = 1 MPa, t_e = 2 ms, (Averaged images obtained by Laser tomography on nozzle 1 with sets of 60 images).

4

Microscopic Spray Angle

The microscopic spray cone angle is defined by the inner angle between two lines beginning at the edges of the nozzle hole exit running through two determined points of the spray boundary at a distance of 2 mm from the nozzle hole exit, which corresponds to the limit of the spray image (image resolution 2μm/pixel).

Figure 8-a shows the evolution of the spray angle according to the needle lift during the injection cycle. We can see that during the needle opening, the explosion of the mushroom due to the Re increase, leads to an increasing spray angle which reaches a maximum at the moment of the cavitation inception in the injection orifice ($K = K_{crit} \approx 1.8$). Just after the inception of the cavitation, K and Re keep on increasing but the Re increase affects more the spray angle. The spray angle decreases in this phase because the relative velocity between the spray and the ambient gas in the outside region becomes larger. When the needle is fully opened, the flow is quasi-stationary, and an approximately constant spray angle is observed. In this phase K and Re are stable. During the needle closing, again a widening of the spray angle occurs due to the Re decrease, and so the influence of the ambient pressure becomes more important on the spray angle. The spray angle reaches its second maximum value when the cavitation begins to be sucked from the injection orifice. Heimgärtner and Leipertz [1] have considered that the evolution of the microscopic angle in dependence on the rail pressure can be fitted by a function of second order (Eq. 3) for single-hole nozzle and when the needle is fully opened.

$$\theta_{micro} = a_1 P_R^2 + a_2 P_R + a_3 \tag{3}$$

Figure 8-b shows that the spray angle increases with the decrease in rail pressure. We have seen before that at full needle lift, the cavitation rate at fixed back-pressure is almost the same for an increasing rail pressure (*cf.* Fig.7-b), whereas Re and consequently the flow velocity, increase considerably (*cf.* Fig.5-a) which causes the decrease of the spray angle. It is shown also in this figure that the spray angle increases with the increase in backpressure. In fact, when the backpressure is increased the exit orifice flow might unchoke and the gradual widening of the spray thereafter could result from the increased drag on drops resulting from greater ambient density. Consequently, θ_{micro} will be a bi variable function of P_R and P_b. So an attempt has been made to take into account the dependence of the coefficients of Eq. (3) on the backpressure thanks to a least square procedure, and we have obtained:

$a_1 = 0.0022\ P_b{}^2 - 0.0078\ P_b + 0.0125$; $a_2 = -0.1366\ P_b{}^2 + 0.4458\ P_b - 0.9167$; $a_3 = 1.8618\ P_b{}^2 - 4.1312\ P_b + 24.807$ (4)

As these parameters are dimensional and that the equation (3) is valid only at full needle lift, we have tried to make an empirical law according to the dimensionless physical parameters Re and K, and which will be valid during the whole injection process. We have obtained the following function:

$$\theta_{micro} = b_1.(Re)^{b_2}.K^{b_3} + b_4.(Re)^{b_5} + b_6.K^{b_7} \tag{5}$$

where $b_1 = 15.13$; $b_2 = -0.05$; $b_3 = -0.20$; $b_4 = 38$; $b_5 = -0.25$; $b_6 = 3.41$; $b_7 = -0.07$; correlation coefficient $R^2 = 88$ %.

Figure 9 shows a comparison of the spray angle evolution calculated by the model and that obtained experimentally. We can see that the larger deviation between the spray angles calculated and those measured experimentally takes place mainly for the first two spray angles and thus for the cases of high rail pressure (Fig. 9-b). This is due that for these cases, besides Re and K effects, a third parameter interferes; it is the explosion of the mushroom which occurs practically at the same time of the cavitation inception and which is a random phenomena and can give rise to the spray angle because of the ligaments detached from the main spray. Whereas for the other points, the model gives a good approximation of the measured spray angles, because in these phases, only Re and K control the flow. It should be noticed that the considered spray angles in the model are taken in the interval between theirs two maxima.
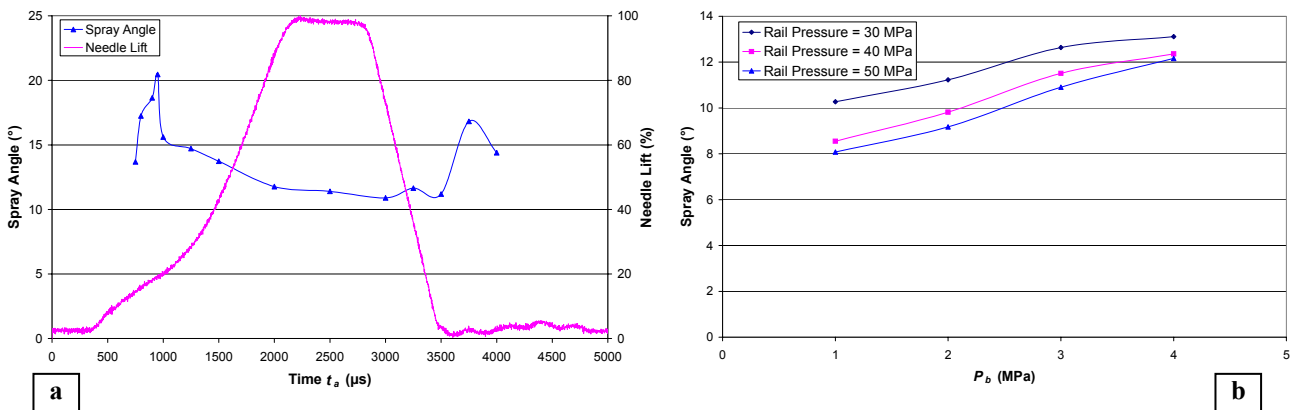

Fig. 8 (a)-Spray cone angle close to the nozzle exit $P_R = 30$ MPa, $P_b = 1$ MPa, $t_e = 2$ ms, (results obtained on nozzle 3) (b)-Influence of rail pressure and backpressure on spray angle, $t_a = 2500$ μs, needle lift at 100 %, (results obtained on nozzle 2).
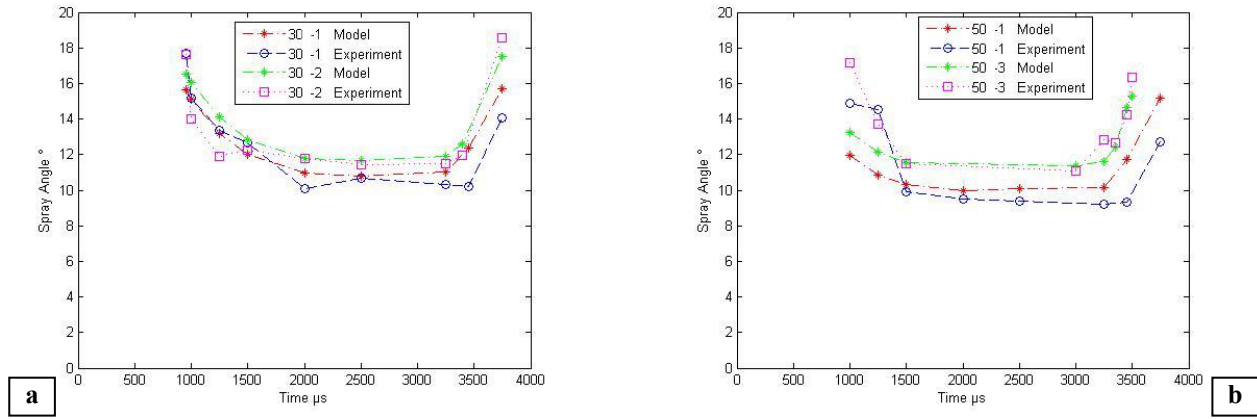
Fig. 9 Comparison of the spray angle evolution calculated by the model (Eq. 5) and the experiment.

CONCLUSION

This study characterises the overall injection process. It points out the natural link between the cavitating nozzle flow and the downstream spray pattern. At the beginning stage of the needle lift, the main stream of the spray shapes like a mushroom and its tip starts to collapse due to the drag. In later stage, at full needle lift, a quasi stationary flow takes place, in which the turbulence has not enough influence to affect the spray angle which remains constant. Nevertheless the spray angle increases with the rail pressures decrease and the backpressure increase. Due to geometrical sac asymmetry, an asymmetric cavitation region occurs in the spray hole as well as an asymmetry spray angle close to the nozzle. In final stage, the atomisation of the spray becomes very poor and larger droplets appear on the edges of the spray. Two empirical functions have been established to calculate the spray angle during the whole injection cycle (transient and quasi-stationary phases), and it was observed two maximum values: at the moment of the inception of cavitation and at the moment of the sucking of the cavitation from the injection orifice.

Further measurements and diagnostics are still needed to obtain a more accurate model. Studies are in progress to find a quantitative link between the cavitation rate in the spray hole and the equivalence ratio in the back-pressure chamber. Visualisations by Laser tomography have to be done in the axial section of the spray to analyse precisely the spray break-up.

NOMENCLATURE

d	Spray hole diameter	(mm)	R^2	Correlation Coefficient		dimensionless
K	Cavitation number	dimensionless	Re	Reynolds number		dimensionless
K_{crit}	Critical cavitation number	dimensionless	S_C/S_T	Cavitation rate		dimensionless
l	Spray hole length	(mm)	t_a	Time after energizing the injector		(µs)
P_b	Ambient back pressure	(MPa)	t_e	Energizing time of the injector		(ms)
P_R	Rail pressure	(MPa)	V	Instantaneous orifice flow velocity		(m/s)
P_s	Nozzle sac pressure	(MPa)	θ_{micro}	Spray cone angle		(°)
P_v	Vaporisation pressure of the fuel	(MPa)	ν	Kinematic viscosity		(m²/s)

REFERENCES

1. C. Heimgärtner and A. Leipertz, Investigation of the Primary Spray Break-up Close to the Nozzle of a Common-Rail High Pressure Diesel Injection System, SAE Paper No. 2000-01-1799, 2000.
2. Bergwerk, W., Flow Pattern in Diesel Nozzle Spray Holes, Proc. Instn. Mech. Engrs, vol. 173, No. 25, pp. 655-660, 1959.
3. Badock C., Wirth R., Fath A., Leipertz A., Investigation of Cavitation in Real Size Diesel Injection Nozzles, International Journal of Heat and Fluid Flow, No. 20, pp. 538-544, 1999.
4. Baz I., Contribution à la Caractérisation de la Cavitation dans les Injecteurs Diesel à Haute Pression, Phd thesis – Ecole Centrale de Lyon, Lyon, France, 2003.
5. M. Blessing, G. König, C. Krüger, U. Michels and V. Schwarz, Analysis of Flow and Cavitation Phenomena in Diesel Injection Nozzles and Its Effects on Spray and Mixture Formation, SAE Paper No. 2003-01-1358, 2003.
6. Goney K., Corradini M., Isolated Effects of Ambient Pressure, Nozzle Cavitation and Hole Inlet Geometry on Diesel Injection Spray Characteristics, SAE Paper No. 2000-01-2043, 2000.
7. E. v. Berg, W. Edelbauer, A. Alajbegovic, R. Tatschl, Coupled Calculation of Cavitating Nozzle Flow, Primary Diesel Fuel Break-up and Spray Formation with an Eulerian Multi-Fluid-Model, Iclass 2003, July 13 – 17, 2003.